Algorithms for iterative phase noise estimation based on a truncated DCT expansion

Jabran Bhatti, Nele Noels and Marc Moeneclaey
Department of Telecommunications and Information Processing
Ghent University, Belgium
Email: {Jabran.Bhatti, Nele.Noels, mm}@telin.ugent.be

***Abstract*—We present two phase noise estimation algorithms for single-carrier burst communications. The first and second estimation techniques (denoted as PEA1 and PEA2 respectively) are based on a truncated discrete cosine transform (DCT) basis expansion of the phase noise and of the corresponding phasor, respectively and do not require any knowledge of the phase noise statistics. An initial pilot-based estimate is iteratively improved by means of the expectation-maximization algorithm, yielding a soft-decision-directed phase noise estimate. The performances of PEA1 and PEA2 are compared in terms of the mean-square phase error and bit-error rate. Numerical results show that PEA2 outperforms PEA1 for practical values of the signal-to-noise ratio.**

I. Introduction

Digital communication systems can suffer significant performance degradation due to the presence of phase noise. Hence, an efficient phase noise estimation technique is of great importance in order to ensure reliable transmission. Phase noise can be estimated by means of a feedback algorithm that operates according to the principle of the phase-locked loop [1], [2], but the long acquisition periods typical of this class of algorithms renders them unsuitable for burst transmission. In [2] and [3], the observation interval is divided into subintervals, and a conventional feedforward algorithm is used to estimate within each subinterval the local time-average (or the linear trend) of the phase. The resulting approximation of the phase noise is accurate only for short subintervals, in which case the sensitivity to additive noise increases. Recently, other estimation algorithms have been proposed [4], [5], however these are computationally rather complex and assume detailed knowledge about the phase noise statistics at the receiver.

We propose a technique based on the basis expansion model, which exploits the low-pass nature of the phase noise process. We use the basis functions from the discrete cosine transform (DCT) to represent the phase noise process; the DCT is known to perform closely to the optimum Karhunen-Loève transform [6]. An estimate of a few of the DCT coefficients is obtained from the received signal. These are used to compute the corresponding phase estimate via the inverse DCT. This contribution covers two phase noise estimation algorithms that apply DCT expansion to the time-varying *phase* $\boldsymbol{\theta}$ and to the corresponding *phasor* $\exp(j\boldsymbol{\theta})$, respectively. In our prior work [7] a phase estimate is obtained from pilot symbols only, via DCT expansion of the phase. Assuming uncoded transmission, the pilot-based algorithm from [7] has been further improved in [8] by also exploiting the energy associated with the unknown data symbols, in an iterative decision-directed setup. Here, we devise the phase estimate applying DCT expansion to the phasor and we compare performances of this algorithm and the algorithm from [8].

The observation model and a general phase noise model are presented in section II. In section III, the two phase noise estimation algorithms are derived, considering both coded and uncoded transmission. Section IV is devoted to the performance analysis of the proposed estimation techniques in terms of the mean-square phase error (MSPE). These analysis results are confirmed by computer simulations in section V. Finally, conclusions are drawn in section VI.

II. System model

Our system assumes transmission of a burst of K symbols over an additive white Gaussian noise (AWGN) channel distorted by phase noise. The observed discrete-time signal samples at the receiver are determined by:

$$r_k = a_k e^{j\theta_k} + w_k, \tag{1}$$

where the index $k = 0, \ldots, K-1$ refers to the $k-$th symbol interval of length T; the additive noise $\{w_k\}$ is a sequence of i.i.d. zero-mean (ZM) circular symmetric complex-valued Gaussian (CSCG) random variables (RVs) with $E[|w_k|^2] = N_0$, and θ_k is the sum of a static phase offset θ_{stat} and a zero-mean phase noise process. The burst contains K_P known pilot symbols at positions $k \in I_P = \{\ k_i,\ i = 0, \ldots, K_P - 1\}$, with constant magnitude: $|a_{k_i}|^2 = E_s$. The remaining $K - K_P$ data symbols are either uncoded (i.e., statistically independent) or coded. They belong to a constellation A, with $E[|a_k|^2] = E_s$ for $k \notin I_P$. For the sake of simplicity, we will consider M-PSK constellations. In the following, we will represent the phase noise vector $\boldsymbol{\theta} = (\theta_0, \ldots, \theta_{K-1})^T$ as a function of a low-pass process $\mathbf{u} = (u_0, \ldots, u_{K-1})^T$. The definition of $\mathbf{u}$ will be specified in section III. Because of its low-pass nature, $\mathbf{u}$ can be well approximated by the weighed sum of a *limited number* $N\,(<< K)$ of discrete cosine transform (DCT) basis functions $\{\psi_{k,n},\ n = 0, \ldots, N-1\}$:

$$\mathbf{u} \approx \mathbf{\Psi_K x}, \tag{2}$$

where $(\mathbf{\Psi_K})_{k,n} = \psi_{k,n}$, $(k = 0, \ldots, K-1;\ n = 0, \ldots, N-1)$ and $\mathbf{x} = (x_0, \ldots, x_{N-1})^T$ is the DCT coefficient vector. Considering (2) as an equality, the phase noise vector $\boldsymbol{\theta}$ can be

viewed as a function of the coefficient vector $\mathbf{x}$, i.e., $\boldsymbol{\theta} = \mathbf{g}(\mathbf{x})$. The orthonormal DCT basis functions are defined as

$$\psi_{k,n} = \begin{cases} \sqrt{\frac{1}{K}} & n = 0 \\ \sqrt{\frac{2}{K}} \cos\left(\frac{\pi n}{K}\left(k + \frac{1}{2}\right)\right) & n > 0 \end{cases}. \quad (3)$$

Note that the n-th basis function contains the frequencies $-n/(2KT)$ and $n/(2KT)$. From the observations (1), the receiver produces an estimate $\{\hat{x}_n, n = 0, \ldots, N-1\}$ of the N DCT-coefficients $\{x_n, n = 0, \ldots, N-1\}$, using the model (2) with equality. The resulting phase estimate is computed as $\hat{\boldsymbol{\theta}} = \mathbf{g}(\hat{\mathbf{x}})$. This phase estimate is used to derotate the received signal before data detection. The detector is designed under the assumption of perfect carrier synchronization, i.e., $\hat{\theta}_k = \theta_k$. For uncoded transmission, the detection algorithm reduces to symbol-by-symbol detection.

III. Estimation algorithms

Since the $K - K_P$ unknown data symbols act as *nuisance* parameters, the estimation of $\mathbf{x}$ is inspired on the expectation-maximization (EM) algorithm. The EM algorithm iteratively produces a sequence of estimates, according to

$$\hat{\mathbf{x}}^{(l)} = arg \max_{\mathbf{x}} E[ln\, p(\mathbf{r}|\mathbf{a};\mathbf{x})|\mathbf{r}, \hat{\mathbf{x}}^{(l-1)}], \quad l = 1, 2, \ldots,$$

where l denotes the iteration number; $p(\mathbf{r}|\mathbf{a};\mathbf{x})$ is the probability density function (pdf) of the received signal $\mathbf{r}$ conditioned on the symbol sequence $\mathbf{a}$, and the DCT coefficient vector $\mathbf{x}$ is considered as an unknown deterministic parameter of this pdf. The natural logarithm $ln\, p(\mathbf{r}|\mathbf{a};\mathbf{x})$ is the *joint log-likelihood function* of $\mathbf{x}$ and $\mathbf{a}$. When the initial estimate is sufficiently accurate, the EM algorithm converges towards the maximum-likelihood (ML) estimate.

A. DCT expansion of the phase

In the first phase estimation algorithm (which, for compactness, we will refer to as PEA1), we simply define $u_k = \theta_k$. Considering (2) with equality, we have $\boldsymbol{\theta} = \boldsymbol{\Psi}_\mathbf{K}\mathbf{x}$. The corresponding observation (1) can be represented as

$$r_k = a_k \exp(j(\boldsymbol{\Psi}_\mathbf{K}\mathbf{x})_k) + w_k. \quad (4)$$

Straightforward application of the EM algorithm yields the following iterative soft-decision-directed (SDD) DCT coefficient vector estimate:

$$\hat{\mathbf{x}}^{(l)} = arg \max_{\mathbf{x}} \sum_{k=0}^{K-1} |r_k \mu_k^{(l)*}| \cos\left(arg(r_k \mu_k^{(l)*}) - (\boldsymbol{\Psi}_\mathbf{K}\mathbf{x})_k\right), \quad (5)$$

where $\mu_k^{(l)} = E[a_k|\mathbf{r}, \hat{\mathbf{x}}^{(l-1)}]$ is the a posteriori expectation of the symbol vector a_k, based on the observation $\mathbf{r} = (r_0, \ldots, r_{K-1})^T$ and the coefficient estimate from the previous iteration. For $k \in I_P$, the symbols a_k are the known pilot symbols, yielding $\mu_{k_i}^{(l)} = a_{k_i}$, for $i = 0, \ldots, K_P - 1$. For $k \notin I_P$, $\mu_k^{(l)}$ represents a soft decision on the data symbol a_k. In the case of uncoded transmission, we get, for $k \notin I_P$:

$$\mu_k^{(l)} = \frac{\sum_{\alpha \in A} \alpha \exp\left(-\frac{1}{N_0}|r_k - \alpha e^{j\hat{\theta}_k^{(l-1)}}|^2\right)}{\sum_{\alpha \in A} \exp\left(-\frac{1}{N_0}|r_k - \alpha e^{j\hat{\theta}_k^{(l-1)}}|^2\right)} \quad (6)$$

where $\hat{\theta}_k^{(l-1)}$ is the phase estimate that corresponds to $\hat{\mathbf{x}}^{(l-1)}$. In the case of coded transmission, the soft symbol decisions are obtained from the marginal a posteriori symbol probabilities $Pr[a_k|\mathbf{r}, \hat{\mathbf{x}}^{(l-1)}]$ that are computed by the decoder; the resulting estimation algorithm is called code-aided (CA). In order to avoid the additional complexity of incorporating the decoder output in the estimation algorithm, one could use (6) also in the case of coded transmission; the resulting estimation algorithm is non-code-aided (NCA), as the code properties are not exploited during estimation.

An initial pilot-based (PB) estimate $\hat{\mathbf{x}}^{(0)}$, required to start the EM iterations (5), is obtained by restricting the summation in (5) to indices k belonging to I_P:

$$\hat{\mathbf{x}}^{(0)} = arg \max_{\mathbf{x}} \sum_{i=0}^{K_P-1} |r_{k_i} a_{k_i}^*| \cos\left(arg(r_{k_i} a_{k_i}^*) - (\boldsymbol{\Psi}_\mathbf{P}\mathbf{x})_i\right) \quad (7)$$

where $(\boldsymbol{\Psi}_\mathbf{P})_{i,n} = \Psi_{k_i,n}$ $(i = 0, \ldots, K_P - 1; n = 0, \ldots, N-1)$.

As the functions to be maximized in (5) and (7) depend on $\mathbf{x}$ in a highly non-linear way, a closed form expression of the estimate of $\mathbf{x}$ is infeasible. Instead, as an alternative to (5), we propose to compute the least-squares estimate $\hat{\mathbf{x}}^{(l)}$ that minimizes $\sum_k |arg(r_k \mu_k^{(l)*}) - (\boldsymbol{\Psi}_\mathbf{K}\mathbf{x})_k|^2$ in [8]. However, as the range of the function $arg(.)$ is limited to $[-\pi, \pi]$, this estimation strategy is susceptible to phase wrapping. Here, we avoid phase wrapping issues by applying phase unwrapping to the function $arg(.)$. In the remainder of this paper, $arg(y)$ denotes the function that returns the unwrapped angle of y. The resulting least-squares estimation of $\mathbf{x}$ yields, for $l > 0$,

$$\hat{\mathbf{x}}^{(l)} = (\boldsymbol{\Psi}_\mathbf{K}^\mathbf{T}\boldsymbol{\Psi}_\mathbf{K})^{-1}\boldsymbol{\Psi}_\mathbf{K}^\mathbf{T}\mathbf{z}^{(l)} = \boldsymbol{\Psi}_\mathbf{K}^\mathbf{T}\mathbf{z}^{(l)}, \quad (8)$$

where $(\mathbf{z}^{(l)})_k = arg(r_k \mu_k^{(l)*})$. The second equality in (8) follows from the orthonormality of the DCT basis functions. The corresponding estimate of $\boldsymbol{\theta}$ is given by

$$\hat{\boldsymbol{\theta}}^{(l)} = \boldsymbol{\Psi}_\mathbf{K}\boldsymbol{\Psi}_\mathbf{K}^\mathbf{T}\mathbf{z}^{(l)}. \quad (9)$$

Similarly, the initial PB phase estimate is given by

$$\hat{\boldsymbol{\theta}}^{(0)} = \boldsymbol{\Psi}_\mathbf{K}(\boldsymbol{\Psi}_\mathbf{P}^\mathbf{T}\boldsymbol{\Psi}_\mathbf{P})^{-1}\boldsymbol{\Psi}_\mathbf{P}^\mathbf{T}\mathbf{z}^{(0)},$$

where $(\mathbf{z}^{(0)})_i = arg(r_{k_i} a_{k_i}^*)$ $(i = 0, \ldots, K_P - 1)$. In order that $\boldsymbol{\Psi}_\mathbf{P}^\mathbf{T}\boldsymbol{\Psi}_\mathbf{P}$ be invertible, we need $K_P \geq N$. Arranging the pilot symbols according to

$$k_i = \frac{K(2i+1) - K_P}{2K_P}, \quad (10)$$

for $i = 0, \ldots, K_P - 1$, yields a diagonal matrix $\boldsymbol{\Psi}_\mathbf{P}^\mathbf{T}\boldsymbol{\Psi}_\mathbf{P}$: $\boldsymbol{\Psi}_\mathbf{P}^\mathbf{T}\boldsymbol{\Psi}_\mathbf{P} = K_P/K\mathbf{I}_\mathbf{N}$ [7], where $\mathbf{I}_\mathbf{N}$ is the $N \times N$ identity matrix. The initial PB estimate is then given by

$$\hat{\boldsymbol{\theta}}^{(0)} = \frac{K}{K_P}\boldsymbol{\Psi}_\mathbf{K}\boldsymbol{\Psi}_\mathbf{P}^\mathbf{T}\mathbf{z}^{(0)}, \quad (11)$$

In the remainder of this paper, we assume the pilot symbols are inserted according to (10).

B. DCT expansion of the phasor

We denote the second phase estimation algorithm as PEA2. The need for phase unwrapping is avoided by estimating the DCT coefficients $\mathbf{x}$ of the phasor rather than of the phase: we take $u_k = \exp(j\theta_k)$. As u_k is complex-valued, $\mathbf{x}$ is complex-valued as well. The corresponding observations (1) can be represented as

$$r_k = a_k(\mathbf{\Psi_K x})_k + w_k. \tag{12}$$

Note that $\mathbf{r}$ is a linear function of $\mathbf{x}$. Straightforward application of the EM algorithm yields, for $l > 0$,

$$\begin{aligned}\hat{\mathbf{x}}^{(l)} &= arg \max_{\mathbf{x}} \left(\mathbf{x}^H \mathbf{\Psi_K}^T \mathbf{v}^{(l)} + \mathbf{v}^{(l)H} \mathbf{\Psi_K x} - \mathbf{x}^H \mathbf{x} \right) \\ &= \mathbf{\Psi_K}^T \mathbf{v}^{(l)},\end{aligned}$$

with $(\mathbf{v})_k^{(l)} = r_k \mu_k^{(l)*}/E_s$ and $\mu_k^{(l)} = E[a_k|\mathbf{r}, \hat{\mathbf{x}}^{(l-1)}]$. The resulting iterative SDD phase estimate is given by

$$\hat{\theta}_k^{(l)} = arg \left((\mathbf{\Psi_K \Psi_K}^T \mathbf{v}^{(l)})_k \right). \tag{13}$$

In the same way, a PB initial estimate is obtained by considering the observations for $k \in I_P$ only. When the pilot symbol positions are given by (10), this yields

$$\hat{\theta}_k^{(0)} = arg \left((\mathbf{\Psi_K \Psi_P}^T \mathbf{v}^{(0)})_k \right),$$

with $(\mathbf{v})_i^{(0)} = r_{k_i} a_{k_i}^*/E_s$ for $i = 0, \ldots, K_P - 1$.

Note that the estimation algorithms only rely on the low-pass nature of the phase noise process, and do not require any specific knowledge about the phase noise statistics.

IV. Performance analysis

As a performance measure of the proposed estimation algorithms, we consider the mean-square phase error (MSPE), which is defined as

$$\begin{aligned}MSPE &= \frac{1}{K} E \left[\sum_{k=0}^{K-1} \left(\hat{\theta}_k - \theta_k \right)^2 \right] \\ &= \frac{1}{K} E \left[\text{trace}((\hat{\boldsymbol{\theta}} - \boldsymbol{\theta})(\hat{\boldsymbol{\theta}} - \boldsymbol{\theta})^T) \right].\end{aligned} \tag{14}$$

As a closed-form expression of the MSPE in terms of the system parameters cannot be obtained, we will instead present here an approximate performance analysis, which includes some simplifying assumptions for the sake of mathematical tractability. Assuming small additive noise and small phase estimation errors after convergence of the iterative estimation algorithms, the soft decisions $\mu_k^{(\infty)}$ after convergence are approximated by the actual data symbols a_k. When evaluating the MSPE, we use the observation model (1), where the actual number of DCT coefficients of $\mathbf{u}$ is not necessarily the same as the number (N) taken into account by the estimation algorithm PEA1 or PEA2. For PEA1, using $\mu_k^{(\infty)} = a_k$ in (9) yields

$$\hat{\theta}_k^{(\infty)} = \sum_{k'=0}^{K-1} (\mathbf{M})_{k,k'} arg(r_{k'} a_{k'}^*), \tag{15}$$

where we have defined $\mathbf{M} = \mathbf{\Psi_K \Psi_K^T}$. For $N_0/E_s << 1$, we obtain the following linearization:

$$arg\,(r_k a_k^*) \approx \theta_k + \Im[n_k e^{-j\theta_k}]. \tag{16}$$

where $\{n_k = w_k a_k^*/E_s\}$ is a sequence of i.i.d. ZM CSCG RVs with $E[|n_k|^2] = N_0/E_s$. Combining (15) and (16) with equality, the linearized phase estimation error resulting from PEA1 is given by

$$\hat{\theta}_k - \theta_k = \sum_{l=0}^{K-1} \left((\mathbf{M})_{k,l} \Im[n_l e^{-j\theta_l}] - (\mathbf{I_K} - \mathbf{M})_{k,l} (\theta_l - \theta_k) \right), \tag{17}$$

where we have dropped the superscript $^{(\infty)}$ for notational convenience. The first term in (17) is caused by the additive noise, whereas the second term in (17) represents the modeling error resulting from considering only N out of K basis functions in the expansion of θ_k. As the rows of $\mathbf{I_K} - \mathbf{M}$ are orthogonal to the columns of $\mathbf{\Psi_K}$, only the projection of θ_k on the subspace that is orthogonal to the columns of $\mathbf{\Psi_K}$ contributes to the phase estimation error. As the columns of $\mathbf{\Psi_K}$ are the N lowest-order DCT basis functions, the matrix operator $\mathbf{I_K} - \mathbf{M}$ can be interpreted as a high-pass filter with cut-off frequency $N/(2KT)$. Similarly, the matrix operator $\mathbf{M} = \mathbf{\Psi_K \Psi_K^T}$ can be viewed as a low-pass filter with cut-off frequency $N/(2KT)$. Hence, making N larger (smaller) increases (decreases) the noise contribution but decreases (increases) the effect of the modeling error.

For PEA2, using $\mu_k^{(\infty)} = a_k$ in (13) yields

$$\begin{aligned}\hat{\theta}_k - \theta_k &= arg \left(1 + e^{-j\theta_k} \sum_{l=0}^{K-1} (\mathbf{M})_{k,l} n_l \right. \\ &\left. - \sum_{l=0}^{K-1} (\mathbf{I_K} - \mathbf{M})_{k,l} e^{j(\theta_l - \theta_k)} \right) \\ &\approx \sum_{l=0}^{K-1} \left((\mathbf{M})_{k,l} \Im[n_l e^{-j\theta_k}] - (\mathbf{I_K} - \mathbf{M})_{k,l} \sin(\theta_l - \theta_k) \right).\end{aligned} \tag{18}$$

The first and second term in the second line of (18) represent the noise contribution and the contribution from the modeling error, respectively. The approximation in (18) holds when these contributions have variances that are much less than 1.

As $\{n_k, k = 0, \ldots, K-1\}$ consists of i.i.d. ZM CSCG RVs, it follows that the noise contributions in (17) and (18) have the same statistical properties. Denoting the contribution of the additive noise to the MSPE from (14) by $MSPE_{noise}$, one obtains

$$MSPE_{noise} = \frac{N_0}{2E_s} \frac{1}{K} \text{trace}(\mathbf{M}\mathbf{M}^\mathbf{T}) = \frac{N_0}{2E_s} \frac{N}{K}. \tag{19}$$

Hence, both algorithms yield the same $MSPE_{noise}$, which is proportional to the ratio N/K; (19) is consistent with the observation that the matrix operator $\mathbf{M}$ acts like a low-pass filter with bandwidth $N/(2KT)$. The terms in (17) and (18) that result from the modeling error give rise to a contribution

to MSPE which we denote $MSPE_\infty$; at large E_s/N_0, MSPE converges to $MSPE_\infty$. We observe from (17) and (18) that the two estimation algorithms yield different modeling error contributions to the phase estimation error, and, therefore, will give rise to different values of MSPE. However, when the approximation $sin(\theta_l - \theta_k) \approx \theta_l - \theta_k$ is valid (e.g., for small phase noise), both algorithms yield essentially the same value of $MSPE_\infty$.

V. Numerical results and discussion

We examine the performance of the proposed phase noise estimation techniques in terms of the MSPE and the resulting bit-error rate (BER) degradation, using computer simulations. We consider transmission of a burst of K QPSK symbols, containing K_P known pilot symbols that are inserted into the data sequence according to (10), over an AWGN channel perturbed by Wiener phase noise. The Wiener model is commonly used to characterize the phase noise behaviour of practical oscillators [4], [9]. The discrete-time Wiener phase noise process is described by the following system equation:

$$\theta_{k+1} = \theta_k + \Delta_k, \text{ for } k = 0, \ldots, K-2. \tag{20}$$

The initial phase noise value θ_0 is uniformly distributed in $[-\pi, \pi]$ and $\{\Delta_k\}$ is a sequence of i.i.d. zero-mean Gaussian random variables with variance σ_Δ^2. Hence, θ_k can be viewed as the output of an integrator with a white noise input. From (20), it follows that the variance of the Wiener phase noise increases linearly with the time index k, indicating that the process is non-stationary.

Numerical results for coded transmission are based on the Digital Video Broadcasting standards for Terrestrial television (DVB-T) and for Satellite services (DVB-S) [10], [11], which support transmission of QPSK symbols encoded by the maximum free distance convolutional code with rate $r = 1/2$ and generators $g_1 = (133)_8$ and $g_2 = (171)_8$. Note that the results relating to the MSPE for coded transmission with NCA estimation are the same as for uncoded transmission, since in both cases, the soft decisions are computed under the assumption of statistically independent data symbols.

Simulations are carried out for $K = 100$, $K_P = 10$ and $\sigma_\Delta = 3°$. Figure 1 compares the simulated MSPE resulting from PEA1 and PEA2 with the linearized MSPE from section IV (denoted as $MPSE_{lin}$). The algorithms are initialized by the PB estimate of the average phase, i.e., $N^{(PB)} = 1$ DCT coefficient is estimated during initialization. For the iterative SDD estimate, we use $N^{(SDD)} = 9$. For high signal-to-noise ratio (SNR), figure 1 shows that - in accordance with the analysis in section IV - the MSPE converges towards the error floor $MSPE_\infty$, which is virtually the same for PEA1 and PEA2. For $E_s/N_0 > 10\,dB$, the MSPE curves coincide with $MSPE_{lin}$. As the SNR decreases, the simulated MSPE starts to diverge from $MSPE_{lin}$. We observe that the deviation is larger and occurs at a higher E_s/N_0-value for NCA phase estimation as compared to CA phase estimation. For CA phase estimation, the decoder output information yields more reliable soft decisions, and the assumption of perfect soft decisions

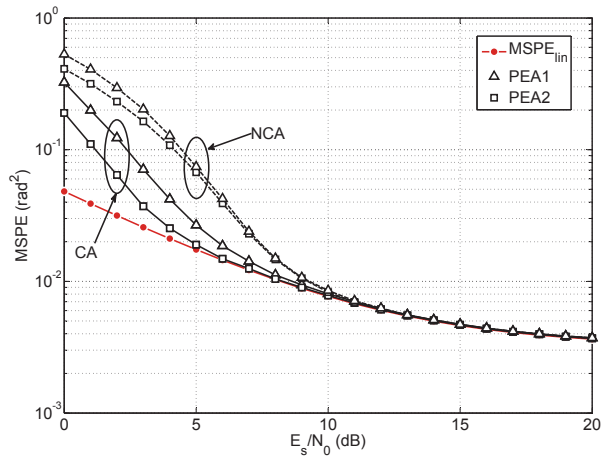

Figure 1. *MSPE as a function of E_s/N_0 with $\sigma_\Delta = 3°$.*

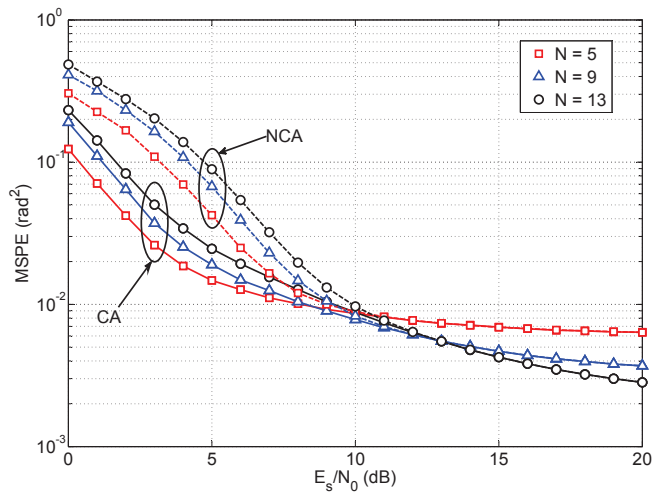

Figure 2. *Influence of N on the MSPE for phase estimation via PEA2 with $\sigma_\Delta = 3°$.*

($\mu_k^{(\infty)} = a_k$) in the computation of the linearized MSPE remains valid for relatively low SNR. We observe that at normal operating E_s/N_0, PEA2 outperforms PEA1 in terms of the MSPE. The influence of the number of estimated coefficients N on the MSPE is illustrated in figure 2 for both CA and NCA phase estimation via PEA2. We may observe that, at high E_s/N_0-values, increasing the number of estimated DCT coefficients improves the performance. Indeed, including more coefficients in the expansion of the phase/phasor reduces the modeling error. In the low-E_s/N_0 region the contribution from the additive noise to the MSPE becomes dominant and we notice the opposite effect: the MSPE increases for larger N. This behaviour is in accordance with the expression for the noise contribution to the MSPE $MSPE_{noise}$ (19) which shows that, by estimating a larger number of DCT coefficients, the phase estimate becomes more sensitive to the additive noise, resulting in a degraded performance. Similar results are

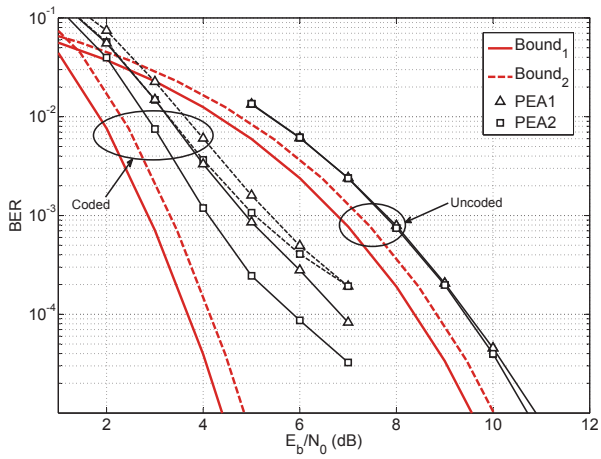

Figure 3. *BER as a function of E_b/N_0 with $\sigma_\Delta = 3°$. For coded transmission, the solid (dashed) lines with markers represent CA (NCA) estimation.*

obtained for PEA1 (not shown here).

Figure 3 examines the BER performance as a function of E_b/N_0 (E_b is the energy per transmitted information bit). The $Bound_1$-curve corresponds to the BER when ideal phase recovery takes place and when no pilot symbols are used. $Bound_2$ is the BER for perfect synchronization when the energy loss due to insertion of pilot symbols is taken into account and shows a degradation of $-10\log_{10}(1-K_P/K) = 0.46\,dB$ as compared to $Bound_1$, for $K_P/K = 0.1$. For uncoded transmission, an initial PB phase estimate with $N^{(PB)} = 3$ is iteratively improved using soft decisions obtained via (6), with $N^{(SDD)} = 9$. We observe that when transmitting uncoded data symbols, the BER for PEA1 degrades only at high E_b/N_0 as compared to the BER resulting from PEA2. At lower values of E_b/N_0, both PEA1 and PEA2 lead to essentially the same BER performance. For coded transmission, the BER is depicted for both CA and NCA SDD iterative estimation with $N^{(SDD)} = 2$. The algorithms are initialized using the PB average phase estimate ($N^{(PB)} = 1$). Comparing PEA1 and PEA2, figure 3 shows that PEA2 clearly performs closer to $Bound_1$. It is also confirmed that taking the decoder output into account significantly improves the BER performance for both PEA1 and PEA2. In accordance with the results for the MSPE, we may conclude that CA phase noise estimation via PEA2 yields superior performance as compared to the other proposed estimation schemes.

VI. Conclusions

We propose two iterative soft-decision-directed phase noise estimation algorithms that exploit the low-pass phase noise process by representing the phase noise through a truncated DCT expansion. In the first phase estimation technique (PEA1), the phase estimate is obtained via a least-squares estimate of a limited number N of DCT coefficients of the *phase* expansion. The second phase recovery method (PEA2) yields a phase estimate based on ML estimation of N DCT coefficients of the *phasor* expansion. The resulting linearized mean-square phase error (MSPE) is shown to consist of two contributions: a noise contribution $MSPE_{noise}$, which is the same for PEA1 and PEA2 and increases with N, and a MSPE floor, caused by neglecting the $K - N$ higher-order DCT coefficients, which decreases as N increases. Numerical simulation results indicate that PEA2 outperforms PEA1, both in terms of MSPE and BER degradation. At common operating SNR, CA phase estimation using PEA2 yields significantly better performance than the other proposed strategies. As an extension of this work, research is ongoing to combine the proposed algorithms with carrier frequency offset estimation.

Acknowledgement

The authors wish to acknowledge the activity of the Network of Excellence in Wireless COMmunications NEWCOM++ of the European Commission (contract no. 216715) that motivated this work. The second author would like to acknowledge the financial support of the Fund for Scientific Research - Flanders (FWO Vlaanderen).

References

[1] N. Noels, H. Steendam, and M. Moeneclaey, "Performance analysis of ML-based feedback carrier phase synchronizers for coded signals," *IEEE Transactions on Signal Processing*, vol. 55, no. 3, pp. 1129–1136, March 2007.

[2] H. Meyr, M. Moeneclaey, and S. Fechtel, *Digital Communication Receivers : Synchronization, Channel Estimation and Signal Processing*. USA: Wiley Series in Telecommunications and Signal Processing, 1998.

[3] L. Benvenuti, L. Giugno, V. Lottici, and M. Luise, "Code-aware carrier phase noise compensation on turbo-coded spectrally-efficient high-order modulations," in *Proceedings of 8-th International Workshop on Signal Processing for Space Communications*, Catania, Italy, September 2003, pp. 177–184.

[4] G. Colavolpe, A. Barbieri, and G. Caire, "Algorithms for iterative decoding in the presence of strong phase noise," *IEEE Journal on Selected Areas in Communications*, vol. 23, pp. 1748–1757, September 2005.

[5] E. Panayirci, H. Cirpan, and M. Moeneclaey, "A sequential Monte-Carlo method for blind phase noise estimation and data detection," in *Proceedings of European Signal Processing Conference (EUSIPCO)*, Antalya, Turkey, September 2005.

[6] T. Ahmed, N. Natarajan and K. Rao, "Discrete cosine transform," *IEEE Trans. Computers*, vol. 23, no. 1, pp. 90 – 93, January 1974.

[7] J. Bhatti and M. Moeneclaey, "Feedforward data-aided phase noise estimation from a DCT basis expansion," *EURASIP Journal on Wireless Communications and Networking, Special Issue on Synchronization in Wireless Communications*, January 2009.

[8] ——, "Iterative soft-decision-directed phase noise estimation from a DCT basis expansion," in *Proceedings of PIMRC 2009*, Tokyo, Japan, September 2009.

[9] S. Bay, C. Herzet, J. Brossier, J. Barbot, and B. Geller, "Analytical and asymptotic analysis of Bayesian Cramer-Rao bound for dynamical phase offset estimation," *IEEE Transactions on Signal Processing*, vol. 56, no. 1, pp. 61–70, January 2008.

[10] ETSI, "EN 300 744 v1.6.1 (2009-01), Digital Video Broadcasting (DVB); Framing structure, channel coding and modulation for digital terrestrial television," 2009.

[11] ——, "EN 300 421 v1.1.2 (1997-08), Digital Video Broadcasting (DVB); Framing structure, channel coding and modulation for 11/12 GHz satellite services," 1997.